research review

OFFICE OF AEROSPACE RESEARCH

OAR: The Research Agency
of The United States Air Force

VOLUME VI NUMBER 8 AUGUST 1967

scattering and energy transfer in the collision of atoms and molecules with metal surfaces

JOE N. SMITH, JR., Atomic Physics Laboratory, General Atomic Division,
General Dynamics Corporation

When a gaseous atom or molecule strikes a solid surface, it may rebound immediately from the local surface element that it strikes, or it may interact strongly with the surface or with other atoms or molecules on the surface prior to re-emission. In the latter case, energy exchange between the gas atom and the surface is to be expected as well as the possibility of molecular dissociation or reconstitution and chemical reaction. If the "residence time" (the time spent by the gas molecule in the region of the surface) is long, the re-emission will tend to be random in direction. In the case of a less strongly interacting gas-surface system, the spatial distribution of the scattered molecules will, in general, be an indication of the dynamical response of the system to the collision, and will depend on the angle of incidence of the molecule upon the surface, the initial energy of the molecule, the temperature of the solid and the intrinsic properties of the system.

A complete knowledge of these various processes is vital in several areas of science and technology, notably the physics of ultra-high vacuum and the aerodynamic forces on flight vehicles at altitudes high enough that molecule-surface collisions predominate over molecule-molecule collisions in the gas phase. For aerodynamic design calculations, it is usually sufficient to have numerical values for the normal and tangential "momentum accommodation coefficients" which describe in macroscopic terms the pressure and shear forces exerted on a surface exposed to a parallel stream of molecules. However, the same information may be obtained from a knowledge of the energy transfer in the gas-surface collision and the direction of re-emission of the gas molecule. Not only is the scattering process easier to study in the laboratory than measuring forces in the microdyne range but, in addition to providing data of aerodynamic interest, this information is of a much more fundamental nature because it yields an insight into the physics of the interaction on the atomic scale.

In 1958, a research program was begun at the General Atomic Division of General Dynamics Corporation, under the direction of Wade L. Fite, to study the interaction of atmospheric-gas species with metal surfaces using modulated atomic and molecular-beam techniques. The present author joined the program in 1959, H. Saltsburg in 1962, and R. L. Palmer in 1965. Since 1963, the re-

AIR FORCE OFFICE of SCIENTIFIC RESEARCH ★ The FRANK J. SEILER RESEARCH LABORATORY
AIR FORCE CAMBRIDGE RESEARCH LABORATORIES ★ AEROSPACE RESEARCH LABORATORIES
OFFICE of RESEARCH ANALYSES ★ EUROPEAN OFFICE, OAR ★ LATIN AMERICAN OFFICE, OAR

search has proceeded under the direction of Smith and Saltsburg. The General Atomic program has been supported by the Mechanics Division of the Directorate of Engineering Sciences, AFOSR, since its inception in 1958.

In the early stages of this research program, scattering, momentum transfer and energy transfer (thermal accommodation), molecular dissociation and recombination, and chemical-reaction studies were performed on various polycrystalline metal-foil targets.(1, 2, 3, 4) Experimentation on these so-called "engineering surfaces" was justified on the basis that they were representative of the materials of technological interest to aerospace development. However, although considerable information did result from these experiments, it became apparent that the lack of a fundamental understanding of molecule-surface collisions prevented the accumulation of useful aerodynamic data. Hence, the direction of research was reoriented toward more basic studies.

Since 1963 the General Atomic group has been studying molecular-beam scattering from the surfaces of metal films produced by vacuum evaporation in situ in the molecular-beam apparatus. By depositing these films on mica maintained at 560°K, single-crystal films of gold and silver have been produced. In addition, by depositing the

research review
OFFICE OF AEROSPACE RESEARCH

OAR RESEARCH REVIEW is published monthly by the Office of Scientific and Technical Information (RRYC), Hq Office of Aerospace Research, USAF, 1400 Wilson Boulevard, Arlington, Va. 22209. The objective of this publication is to make a positive contribution to the exchange of information concerning Air Force conducted and sponsored research activities.

JACOB SEIDEN
Editor

SCATTERING AND ENERGY TRANSFER IN THE COLLISION OF ATOMS AND MOLECULES WITH METAL SURFACES
Joe N. Smith, Jr. 1

AFCRL TO LAUNCH FOUR ADDITIONAL VOYAGER BALLOONS
Aerospace Instrumentation Laboratory, AFCRL..... 6

THE IMPULSIVE ACCELERATION OF PLASMA
Major Russell G. Langlois..... 7

THE INFLUENCE OF AGING ON THE LOW–TEMPERATURE YIELD POINT IN IRON
Attwell M. Adair..... 9

SOLAR MONITORING SATELLITE LAUNCHED
Space Physics Laboratory, AFCRL..... 11

DETERMINING OVER–ALL REACTION KINETICS OF PROPELLANT SYSTEMS IN A NEW–TYPE FLOW REACTOR
Dr. Bernard T. Wolfson 12

HIGH–ALTITUDE TETHERED BALLOONS
Thomas Kelly..... 14

ATMOSPHERE IN A COMPUTER
Upper Atmosphere Physics Laboratory, AFCRL..... 15

THE LASER AS A LIGHT SOURCE FOR STUDYING IMPERFECTIONS IN CRYSTALS
Capt. Richard C. Powell..... 16

ISOBARIC SPIN––ITS INFLUENCE ON RESEARCH IN NUCLEAR PHYSICS WITH SMALL ACCELERATORS
Dr. Gale I. Harris..... 20

APPLICATION OF HIGH–SPEED HOLOGRAPHIC PHOTOMICROSCOPY
Everett D. Stephens..... 25

DISTRIBUTION OF THIS DOCUMENT IS UNLIMITED

For sale by the Superintendent of Documents, U.S. Government Printing Office Washington, D.C. 20402 - $2.75 per year domestic, 75 cents additional for foreign mailing, 25 cents per single copy and 15 cents per Annual Index. Back issues will not be furnished.

metal continuously at a rate which was large when compared to the vacuum background gas impingement rate, a clean surface was always exposed to the molecular beam. Scattering studies on the surfaces of these clean, single-crystal films remove much of the uncertainty in interpretation associated with the lack of knowledge of the condition of the target surface, as was the case in much of the earlier work.

One of the first explicit demonstrations of the effects of surface contamination on neutral beam scattering was made with the use of continuously deposited gold targets, and is shown in Fig. 1. The ordinate in the figure

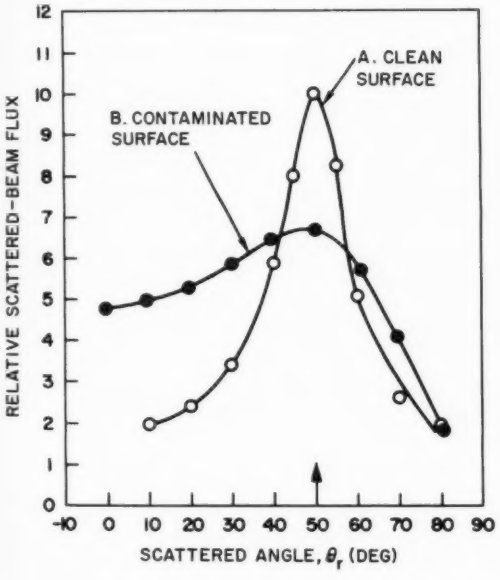

Figure 1. Helium scattering from the (111) plane of gold.

is the relative scattered beam flux, as a function of scattered angle, θ_r, measured in the incident plane (that plane containing the incident beam and the target normal). Curve A is the distribution of a helium beam scattered by the (111) plane of gold, obtained during the gold deposition (i.e., under clean-surface conditions). The scattered beam here is quite narrow and directed toward the specular angle ($\theta_r = 50^o$). Curve B was obtained some time after the cessation of the gold deposition and subsequent contamination of the surface by the ambient vacuum background gas (at a pressure of 5×10^{-7} Torr). Although the beam is still directed in the specular direction, considerable broadening has resulted. Under similar conditions, argon is less strongly affected. (5) Qualitatively, the greater the momentum of the incident atom, the less sensitive is the collision to the presence of an adsorbate. (6) For silver films, effects similar to those depicted in Figure 1 are not observed; i.e., the scattering behavior is the same both during and after evaporation. The binding of adsorbed gases to the silver surfaces may be expected to be stronger than to the gold surfaces, thereby resulting in a more rigid adsorbed structure in the case of silver, one which would absorb energy from the incident gas atom less readily. Although other explanations for the differences in behavior between gold and silver exist, this lattice-like behavior of the contaminant layer on silver as compared with the mattress-like behavior on gold is the most plausible explanation. (7)

For a clean surface, the changes in the scattering behavior produced by a change in the crystal structure of the target are even more dramatic. In Figure 2 is shown the scattering of helium from the clean surface of a polycrystalline gold film (Curve A), and from a smooth single-crystal gold film (Curve B). In the former case, the scattering is completely diffuse (scattered-beam intensity proportional to cosine θ_r), while from the (111) plane the scattering is again specularly directed as in Figure 1. The diffuse scattering here is to be associated with multiple collisions with the rough features of the polycrystalline surface. Obviously, for a partially recrystallized surface, such as a heat-treated metal foil, a behavior intermediate between that depicted by Curves A and B is to be expected. Indeed, that is what was observed in earlier work. (4)

Experimental observations of the directed scattering of argon and xenon from silver single crystals show a behavior that may have considerable significance in the design of orbital and re-entry vehicles. For xenon, this behavior is indicated in Figure 3, which

again shows the scattered-beam distribution at several beam temperatures. When the beam is colder than the surface, the scattered beam is located between the target normal and the specular angle. As the incident beam is heated (with the target temperature held constant), the scattered beam moves away from the normal until, at high temperature, the scattered beam lies between the specular angle and the surface of the target. Aerodynamically speaking, this latter type of scattering (dubbed "supraspecular" by the General Atomic group) would greatly reduce the drag on a surface in free molecule flow. Supraspecular scattering has only been observed for cases in which the temperature of the beam exceeds that of the target. Qualitatively, the behavior shown in Figure 3 may be described in terms of a simple classical model in which no change in tangential momentum occurs. For a "cold" beam, energy transfer increases the normal components of momentum, forcing the beam back toward the target normal. For a "hot" beam, energy is lost in the normal component and the scattered beam falls below the specular angle, toward the surface. Although this concept is greatly oversimplified, it has worked well in describing experimental results, particularly as expanded in the analysis of Logan, Keck, and Stickney. (8)

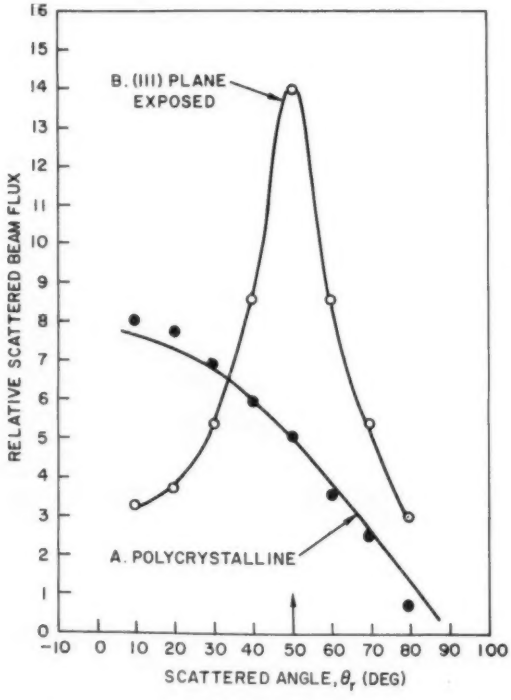

Figure 2. Helium scattering from clean gold.

With the exception of heat-transfer phenomena, the contribution of the internal degrees of freedom (vibration and rotation) of diatomic and polyatomic molecules to the molecule-surface collision process has been ignored. However, recent experiments at General Atomic have indicated that rotational energy exchange may indeed appreciably affect the trajectories of the scattered molecules. These experiments consisted of a high-angular-resolution study of the scattering of helium, hydrogen, and deuterium from the (111) plane of silver. (9) For hydrogen and deuterium the interaction between the molecule and the metal surface is very nearly the same, and differences in scattering behavior between these two gases are obtained which are too great to be attributed to the mass difference. However, the rotational energy-level spacing in deuterium is only one half as big as for hydrogen; in fact, the ground-

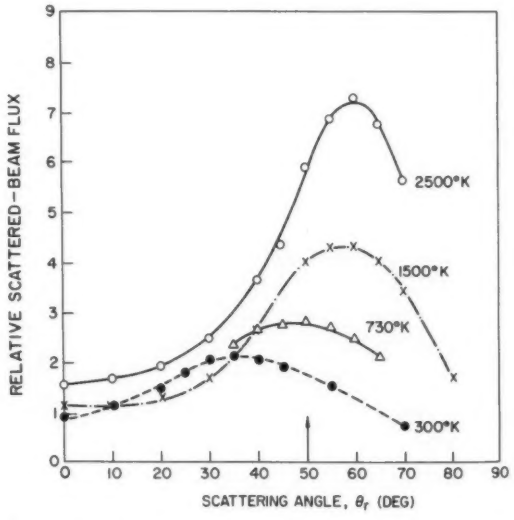

Figure 3. Xenon scattering from the (111) plane of silver as a function of beam temperature. Surface temperature is 560°K and specular angle is $\theta_r = 50°$.

state transition (K = O→2) in orthodeuterium is just 516 cal/mole as compared with the maximum bulk phonon energy of ~450 cal/mole available from the silver lattice, indicating the possibility of a near-resonant condition for deuterium, but not for hydrogen. Theoretical evidence for such coupling between internal and translational energy states is found in the quantum mechanical analysis of Feuer. (10) To shed further light on this question experimentally, the General Atomic group is presently employing a rotating disc velocity selector to fix the kinetic energy of the incident beam, while varying the beam-source temperature to change the internal energy of the molecules. (11) Differences in scattering behavior observed in this way may then be attributed unambiguously to the internal energy content of the incident molecule.

In summary, these experiments, while of a very fundamental nature, are generating considerable information which will permit the development of adequate theory and the concomitant ability to predict the behavior of real systems in the aerospace environment.

REFERENCES

(1) *Hollister, G., R. T. Brackmann and W. L. Fite, "The Use of Modulated Atomic-Beam Technique for the Study of Space Flight Problems," Physical Chemistry and Space Flight, Pergamon Press, 1960, p. 162.*

(2) *Smith, Jr., J. N. and W. L. Fite, "Reflection and Dissociation of H_2 on Tungsten," J. Chem. Phys., 37, 1962, pp. 898-904.*

(3) *Smith, Jr., J. N. and W. L. Fite, "Recent Investigations of Gas-Surface Interactions Using Modulated Atomic-Beam Techniques," Rarefied Gas Dynamics, 1, New York: Academic Press, 1963, pp. 430-453.*

(4) *Smith, Jr., J. N., "Scattering of Atomic Beams by Polycrystalline Nickel," J. Chem. Phys., 40, 1964, pp. 2520-2527.*

(5) *Smith, Jr., J. N. and H. Saltsburg, "Atomic-Beam Scattering from Expitaxially Grown Gold Films," J. Chem. Phys., 40, 1964, pp. 3585-3591.*

(6) *Smith, Jr., J. N. and H. Saltsburg, "Recent Studies of Molecular-Beam Scattering from Continuously Deposited Gold Films," Rarefied Gas Dynamics, 2, New York: Academic Press, 1966, pp. 491-504.*

(7) *Saltsburg, H. and J. N. Smith, Jr., "Molecular-Beam Scattering from the (111) Plane of Silver," J. Chem. Phys., 45, 1966, p. 2175.*

(8) *Logan, R. M., J. C. Keck and R. E. Stickney, "Simple Classical Model for the Scattering of Gas Atoms from a Solid Surface," Rarefied Gas Dynamics, 1, New York: Academic Press, 1967, pp. 49-66.*

(9) *Saltsburg, H., J. N. Smith, Jr. and R. L. Palmer, "Scattering of Molecular Beams of He, D_2, and H_2 from the (111) Plane of Ag," Rarefied Gas Dynamics, 1, New York: Academic Press, 1967, pp. 223-238.*

(10) *Feuer, P., "Theory of the Thermal Accommodation Coefficients of a Diatomic Gas," J. Chem. Phys., 39, 1311, 1963.*

(11) *Saltsburg, H., J. N. Smith, Jr. and R. L. Palmer, "Velocity Selected Molecular-Beam Scattering from the (111) Plane of Silver," Bull. Am. Phys. Soc., 12, 118, 1967.*

Mr. Joe N. Smith, Jr., has been a Staff Member of the Atomic Physics Laboratory, General Atomic Division, General Dynamics Corporation since receiving his B.S. and M.S. degrees at the California Institute of Technology in 1959. He is the principal investigator in the research summarized in this report and sponsored by the Mechanics Division, Directorate of Engineering Sciences, AFOSR (OAR).

AFCRL to launch four additional Voyager balloons

AEROSPACE INSTRUMENTATION LABORATORY, AFCRL

Four mammoth balloon systems, the largest ever developed by this country--815 feet long--will be launched this summer by AFCRL for NASA to test the parachute systems for the Voyager Mars landing vehicle. Tests will be made from Walker Air Force Base, Roswell, New Mexico.

The flights of these 26-million-cubic-foot balloons--scheduled for July and August--will complete the series of 5 balloons for the final selection of the parachute configuration to be used for soft landing the Voyager capsule on Mars in the early 1970's. The first balloon flight in the series of parachute tests was made August 1966, also from Walker Air Force Base.

Except for modifications to the rocketry of the aeroshell used for the parachute tests, and an increase of 100 pounds in the aeroshell's total weight, the tests will be conducted as before. Following each launch, each balloon will drift westward for about 3 hours and a distance of 100 miles until it achieves the desired float altitude of about 130,000 feet over the White Sands Missile Range. A ground command from AFCRL's permanent balloon-launch station at Holloman Air Force Base will trigger the release of the capsule from the balloon.

Seconds after dropping from the balloon, 8 rockets will be ignited to propel the flight unit upward into an arching trajectory, peaking at about 140,000 feet. The new configuration of 8 slightly larger but more powerful rockets will provide an even greater velocity than the previous speed of Mach 1.2 to Mach 1.6, or about 1,100 miles an hour. Under these conditions at high altitude, the velocities and pressures to be achieved will closely correspond to those of a capsule descending through the rarefied Martian atmosphere. When such conditions are reached, a test parachute will be deployed.

The balloons to be used in the coming tests have novel design features. Each is constructed as a two-part interconnected system with the main balloon surmounted by

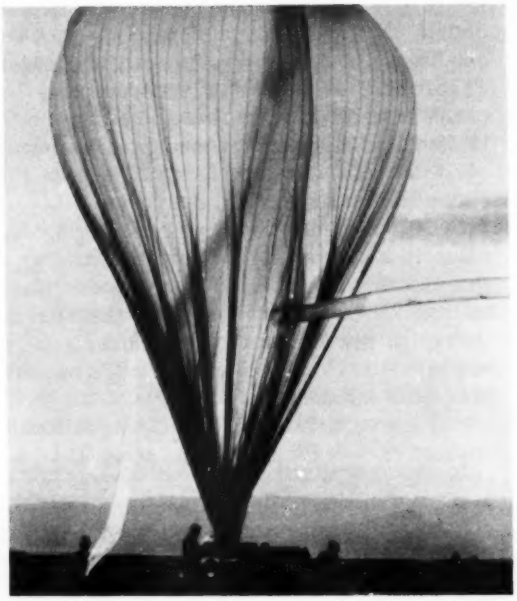

a small launch balloon. Only the small upper balloon is inflated on the ground. During the critical inflation-and-launch stage, the large main balloon remains reefed in a protective sleeve. The two-balloon system also enables easy handling and control of the extremely large balloon train. During prelaunch operations, the top bubble can be tethered near the ground. Just before launch, the entire system is allowed to stand erect, held to the vertical by cables. The main balloon, still reefed at this point, presents a minimum profile to ground winds. Once the launch begins, an anchoring cable attached to the reefing sleeve pulls a rip panel from the sleeve, in a zipper fashion, freeing the main balloon. As the entire system ascends, gas from the upper balloon increases in volume and expands into the main balloon.

The launch of the balloons, their control during flight, and their recovery are managed by AFCRL. Mr. James C. Payne of AFCRL's Aerospace Instrumentation Laboratory is the test director for all of the Voyager balloon flights. The balloons are fabricated by the G. T. Schjeldahl Company of Northfield, Minnesota.

THE IMPULSIVE ACCELERATION OF PLASMA

MAJOR RUSSELL G. LANGLOIS, Directorate of Engineering Sciences, AFOSR

Because of its importance in electric propulsion and thermonuclear fusion studies, the acceleration of a highly ionized plasma by the impulsive application of a strong magnetic field has attracted attention for the past 10 years. The fundamental concept is similar to that of the electric motor. When a current-carrying wire is subjected to a magnetic field, it experiences a Lorentz force, the so-called $J \times B$ force. These ideas apply to the plasma accelerator, except that the conducting plasma is substituted for the wire. Moreover, since the plasma consists of ions and electrons, it is not rigid. Electrons and ions therefore will describe trajectories during the over-all acceleration process depending on circuit parameters and initial conditions. In the case to be described, the orbits of the ions are comparable to the size of the accelerator.

The devices being studied cover a wide variety of geometrics. In some the fields are stationary, while in others the fields move through the accelerator. Some employ electrodes to drive the current, while others are purely inductive. All of them, however, have the common feature of a current-carrying plasma immersed in a strong magnetic field such that the field gradient through the plasma is supported by the plasma current and the resulting force produces acceleration of the plasma mass.

Under AFOSR sponsorship, C. L. Dailey of TRW Systems has been investigating the phenomena associated with an inductively driven plasma accelerator. (1) It is the object of this study to understand the acceleration process and provide a basis for further development of useful plasma thrusters and injection devices. The experimental work is being done in a pulsed, inductive device such that plasma collisions with the wall are avoided. This geometry also simplifies the taking and interpretation of data.

The accelerator coil is a flat-edged, wound spiral having constant current density. When current is pulsed through this coil, it produces a thin, flat layer of plasma current in

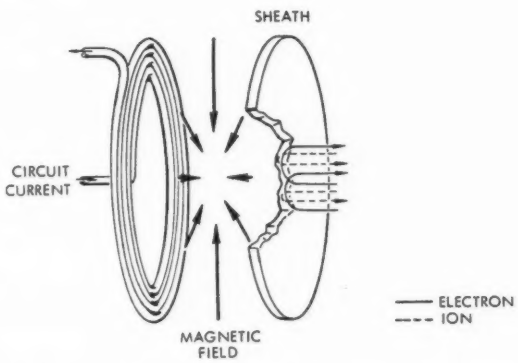

Figure 1. Schematic of collisionless interaction of plasma with cusp field.

which the current density is constant. The magnetic-field shape is a cusp. (See Figure 1.) The most striking feature of this scheme is that a large fraction of the current in the accelerating current layer is carried by the ions. This means that the ions are circulating azimuthally in addition to their axial acceleration away from the plane of the coil. The circulating ion motion arises from the same induced electric field that drives electron current through the plasma in this direction. Evidently the ions act to some extent as if there were no electrons present so that the resultant plasma current is the combination of an ion current and an electron current. Because the ions are heavier, their current lags the electron current so that a composite layer results consisting of an electron-current leading edge followed by a region of ion current.

The mass of ions rotating around the accelerator axis carries angular momentum. The source of this momentum is the induced

azimuthal component of the resultant helical electrical field; the reaction torque is carried back to the coil along these electric-field lines.

Most of the circular ion velocity is converted to axial motion as the ions leave the accelerator. The reason for this is that the resultant magnetic field in the current layer is nearly radial and the ions gyrate around these radial lines as they move axially. However, the scale of the motion for this natural mode of the accelerator is such that the ions execute only the first half-cycle of a gyration by the time they leave the region of influence of the accelerator coil, i.e., an ion moves as if the radial magnetic-field line were a discus thrower. (See Figure 2.)

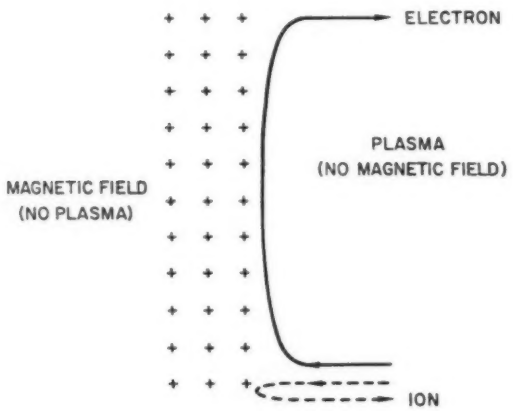

Figure 2. Charged-particle trajectories for a collisionless electron-ion sheath.

The electron-current leading edge of the composite current layer performs the important task of ionization. It also determines the velocity of the accelerated plasma. There are two reasons for this. The first is that the toe of the magnetic field slips through the initially stationary gas at a speed such that the induced electric field can drive the electron current at the power level needed to reach and maintain equilibrium between the rates of ionization and recombination. The second reason is that accelerating forces continue to act on the ions until the plasma mass has been accelerated to the velocity of the electron-current region of the moving magnetic field.

Recent measurements indicate that the induced electric field in the electron-current region is equal to the polarization electric field that transfers the accelerating force of the electron current to the massive ions. This condition of equal electric fields appears to be characteristic of the normal mode of operation. It establishes a simple physical restraint from which the current layer velocity can be related to the recombination coefficient of the gas and the electron temperature.

An impressive demonstration of this property is the fact that altering the gas pressure over a decade and the voltage by a factor of two had no effect on the final velocity of the current layer.

The role played by ion current, that has been identified in the pulsed inductive accelerator, shows that plasma rotation is an inherent feature of the acceleration mechanism. This suggests an induced electric-field mechanism for the plasma rotation that has been observed in theta-pinch geometries, (2, 3, 4) rather than a $J \times B$ body force mechanism as has been suggested by others. (3) Further, an analogous mechanism would explain the ion current found in coaxial guns (5) as corresponding to radial motion of the ions resulting from the radial applied electric field. The accelerated ions would attempt to orbit around the azimuthal magnetic-field lines, as in the pulsed inductive accelerator, but would collide with the coaxial walls in order to provide the required electrode current in that geometry.

REFERENCES

(1) *Dailey, C. L., Proceedings International Astronautical Congress, Madrid, Spain, 9 Oct 1966.*

(2) *Kolb, A. C. et al., Nucl. Fusion Suppl., Pt. 2, 553, 1962.*

(3) *Bodin, H. A. B. et al, Nucl. Fusion Suppl., Pt. 2, 521, 1962.*

(4) *Little, E. M., W. E. Quinn and F. L. Ribe, Nucl. Fusion Suppl., Pt. 2, 497, 1962.*

(5) *Lovberg, R. H., General Atomic/General Dynamics Report GA-4363, June 28, 1963.*

THE INFLUENCE OF AGING ON THE LOW-TEMPERATURE YIELD POINT IN IRON

ATTWELL M. ADAIR, Metallurgy and Ceramics Research Laboratory, ARL

The origin of the low-temperature yield point in metals, also called the transient yield point, is attributed to the interactions of dislocations relaxing back along glide planes during load removal, and is independent of yield effects associated with the influence of impurity atoms. This yield point has been investigated in detail in the face-centered cubic metals and alloys, but little effort has been placed on the characterization of this phenomenon in body-centered cubic metals. The research at ARL a few years ago by Adair and Hook (1) was the first to systematically study this phenomenon in a body-centered cubic metal. Using a vacuum-melted iron, we showed the dependence of this yield point on testing temperature, strain rate, and amount of plastic strain. We also observed a much larger transient yield point following an aging time of one hour at a temperature higher than the testing temperature, and we suggested that it could result from a weak pinning of dislocations by deformation-produced point defects. Further research at ARL has determined the aging response of the transient yield point in iron, and the observed kinetics were examined for an indication of the diffusion of deformation-produced point defects.

Specimens were tested at a temperature of 148°K, and aging was conducted at 148°, 173°, 198°, 223°, and 242°K. Aging times ranged from 10 minutes to 8 hours, with a few exceptions. The transient yield point was observed at 5 strain intervals of 2 percent each, beginning at the 8-10 percent interval. Aging was conducted between these intervals of testing under a minor load to preserve alignment. The transient yield point, $\Delta\sigma$, is expressed in psi and is defined by the drop in load at each strain interval divided by the original cross-sectional area.

The behavior of the transient yield point under immediate reloading conditions (zero aging time between strain intervals) is shown in Figure 1. The linear dependence of $\Delta\sigma$

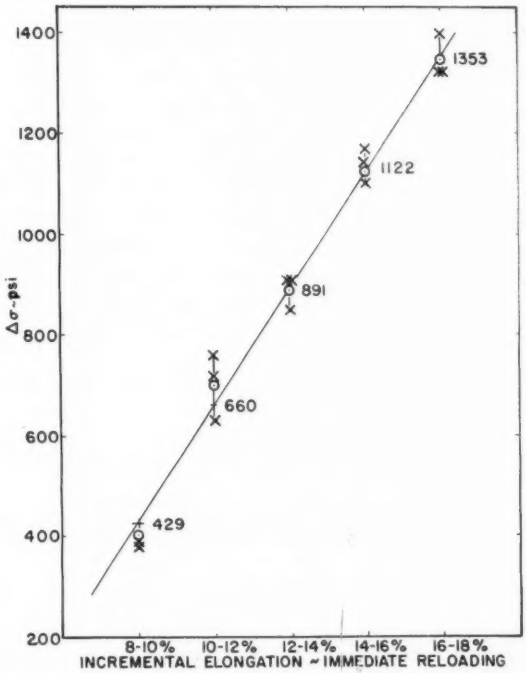

Figure 1. Behavior of transient yield point under immediate reloading conditions (zero aging time between strain intervals).

on the amount of strain results from the increased dislocation density with strain, and is independent of time. These values of $\Delta\sigma$ were subtracted from the total yield point after aging at the corresponding strain interval to give the magnitude of the yield point due to aging, $\Delta\sigma_A$.

The value of $\Delta\sigma_A$ was found to increase logarithmically with aging time for all aging temperatures; however, $\Delta\sigma_A$ was much more dependent on the aging temperature than on aging time. This behavior is shown in Figure 2, where the data points are averages of at least three separate tests for each aging time and temperature.

No kinetics were observed which could be correlated with the diffusion of deformation-produced point defects. The logarithmic increase of $\Delta\sigma_A$ with time at each aging temperature is attributed to additional dislocation

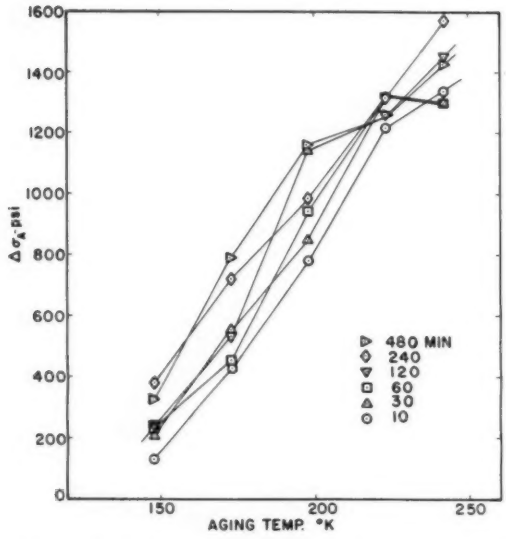

Figure 2. $\Delta\sigma_A$ increases logarithmically with aging time for all aging temperatures, but depends more on aging temperature than on aging time.

relaxation and interaction aided by thermal activation. The strong dependence of $\Delta\sigma_A$ on aging temperature is considered to be a consequence of the temperature dependence of the flow stress for iron. Since the flow stress rapidly decreases with decreasing temperature, the flow stress at the 148°K testing temperature is greater than at the higher aging temperatures. Upon reaching the aging temperature, the dislocations should relax almost immediately to a configuration representative of that temperature. Thus, independent of aging time, this additional relaxation would increase the strength of the barrier to the resumption of plastic flow at the testing temperature, resulting in larger values of $\Delta\sigma_A$. A detailed analysis of the dislocation structures is planned, making use of electron transmission microscopy techniques.

REFERENCES

(1) Adair, A. M. and R. E. Hook, "Yield Points in Iron Upon Reapplication of Load at Low Temperatures," Acta Met., 11, 81, 1963.

Mr. Attwell M. Adair, a physical metallurgist with the Metallurgy and Ceramics Research Laboratory, ARL received his B.S. in Metallurgical Engineering in 1952 from the University of Kentucky, and his M.S. in Metallurgy in 1954 from the Ohio State University. During his graduate training at Ohio State, he conducted research on boron steels. At ARL, he is currently responsible for planning and conducting basic research on the factors influencing the mechanical properties of metals and alloys. Mr. Adair is a member of Tau Beta Pi, Pi Mu Epsilon, the American Society for Metals, and the Metallurgical Society of AIME. He has a number of publications for his credit.

Solar Monitoring Satellite Launched

SPACE PHYSICS LABORATORY, AFCRL

A small, 20-pound satellite was launched by AFCRL on 28 April 1967 into a highly elliptical orbit taking it well beyond the earth's magnetic field. The satellite, designated the OV5-1 and designed to monitor variations in solar radiation, has a 111,000-km apogee and an 8,500-km perigee.

The octahedral satellite (Figure 1), 16 inches tall, was one of 5 Air Force satellites placed in orbit by a single Titan III-C launch vehicle. Excellent data (about 6 hours of data each day) are being received over the satellite's 47.2-hour orbit that takes it alternately into and out of the earth's magnetosphere. The limit of the magnetosphere on the day side is about 65,000 km; on the night side of the earth, the ill-defined limit extends well beyond the moon.

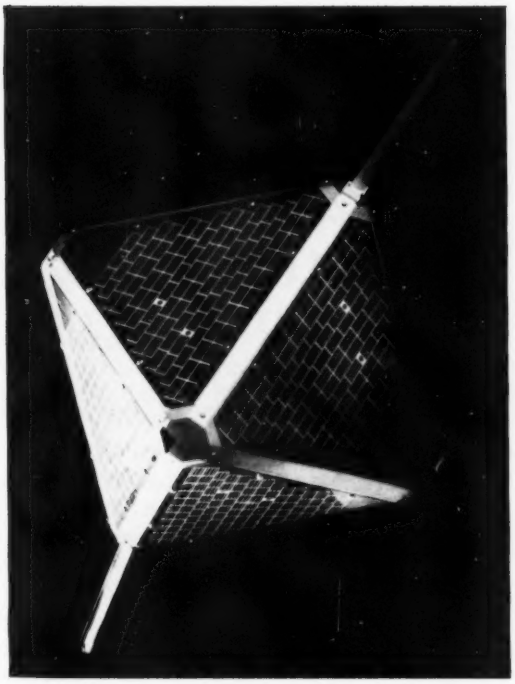

Figure 1. AFCRL's OV5-1 satellite.

The data gathered by the satellite may provide clues to the prediction of solar-induced changes in the earth's aerospace environment. More particularly, the data may help in forecasting the onset of hazardous solar protons emanating from solar flares. The satellite is planned as one in a possible series of solar monitoring satellites, with a successor already proposed for launch soon after the end of the expected one-year lifetime of the OV5-1.

Data are being received at AFCRL's North Ipswich telemetry site in Massachusetts where a 60-foot dish antenna is used to collect the telemetered information. AFCRL is working closely with the Air Weather Service in the over-all environmental forecasting program of which the satellite is a part. AWS observers at the Ipswich site provide satellite data on relative increases in solar-flux values to the AWS Solar Forecasting Center at Cheyenne Mountain, Colorado. Data are also used by AFCRL's Space Forecasting Working Group for interpretation and correlation with other research programs related to environmental forecasting.

The satellite transmits at a frequency of 136.38 MHz. It carries the following instruments: Geiger-Mueller tubes for detecting soft X rays emitted by active solar regions; a low-energy photomultiplier detector for measuring trapped particles in the outer regions of the magnetosphere; a high-energy PM detector for measuring particles in the inner regions and outside the boundary of the magnetosphere; a Bremsstrahlung detector for measuring Bremsstrahlung X rays in the 20- to 100-Kev energy range emitted from active solar regions; a solid-state detector for measuring fluxes of electrons and protons within the magnetosphere and solar protons outside the magnetosphere; and a surface barrier detector for measuring low-energy protons outside the magnetosphere.

The concept for this satellite originated at AFCRL. Major Ronald Bena, Chief of AFCRL's Space Forecasting Branch, is project officer for the satellite. Dr. G. Kenneth Yates is the project scientist.

Major Ronald A. Bena, Chief of the Space Forecasting Branch, Space Physics Laboratory, AFCRL, received a B.A. from St. Louis University in 1952, a B.S. in Electrical Engineering from the Air Force Institute of Technology in 1960, and an M.S. in Electrical Engineering from the University of Missouri in 1964. Upon reporting to AFCRL in September 1960, he was assigned to the Programs Division as Manager of the AFCRL Rocket and Satellite Program. He held this position until July 1966, when he was appointed to his present post.

determining over-all reaction kinetics of propellant systems in a new-type flow reactor

DR. BERNARD T. WOLFSON
Directorate of Engineering Sciences, AFOSR

A new-type flow reactor for the study of homogeneous gas-phase reaction kinetics at high temperatures has been developed by Dr. I. Glassman and his co-workers (in the Guggenheim Propulsion Laboratories of Princeton University) under AFOSR sponsorship. This reactor has been successfully applied to various propellant systems, and has contributed much practical information as well as fundamental kinetic data.

In principle the apparatus consists of a tubular duct in which a high-temperature, turbulent stream of inert gas flows. A secondary cold stream of reactant is introduced into, and mixed rapidly, with the inert gas. Downstream of the injection point reaction commences and continues until all the reactants have been consumed. By varying the velocity of the inert gas, the reaction zone

may be extended over any desired length. The kinetics of more complex reaction systems may be studied by injecting one reactant in the inert gas before the primary mixing point.

By introducing only a small quantity of reactants compared with the mass flow of the carrier, the decrease in temperature resulting from the mixing of the two streams is small--and likewise the increase in temperature due to exothermic reaction will also be relatively small. (Endothermic decomposition reactions which give a subsequent decrease in temperature may be studied in the scheme as well.)

Because the zone in which the reaction takes place is large and the temperature gradient small, such factors as the heat transfer to the unreacted gas and the back diffusion of active species which are dominating effects in self-propagating flames are rendered negligible. In this way an unambiguous determination of reaction kinetics in inerts is possible.

The main duct used in the apparatus at Princeton is constructed of quartz, and can be varied from 1 to 4 inches in diameter (in order to determine heterogeneous wall effects). The inert gas is heated by a packed ceramic bed. A nozzle is used in the injection zone to facilitate mixing. The course of the reaction is followed by means of an axially traversing probe carrying at its tip a Pt/Pt-Rh thermocouple constructed of 0.001-in. wires coated with silica. (The cold junction of the thermocouple is placed in the inert gas prior to the reactant injection point so that the out-of-balance EMF is due solely to the heat release from chemical reaction.) Since the temperature profile across the duct is flat due to the turbulent flow and secondary heating of the quartz duct, a simple longitudinal traverse of the probe provides a record of the temperature change through the reaction zone from which the reaction can be determined. A range of about 50°K is usually covered in any single experiment; however, the apparatus is capable of operating from 900-1,300°K.

Type temperature profiles with and without reaction are shown in Fig. 1. The specific

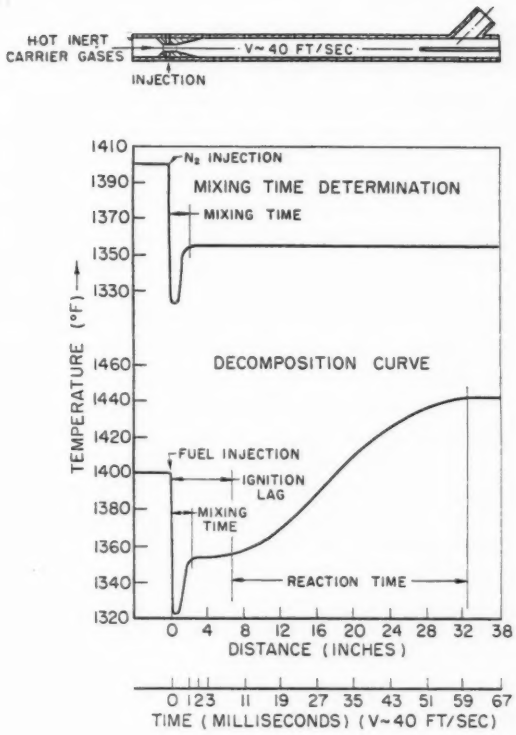

Figure 1. Reactor Temperature Profiles.

reaction-rate constant k is determined from the law of mass action and thermochemistry in the following manner (simplified for purposes here to the study of a first-order reaction):

$$-\frac{dc}{dt} = kc$$

$$cQ = \overline{c_p}\ (T_f - T)$$

$$\frac{1}{(T_f - T)}\frac{dT}{dt} = \frac{1}{(T_f - T)}\, v\, \frac{dT}{dx} = k = Ae^{-E/RT}$$

where c is the concentration at any point, T and v the corresponding temperature and velocity, T_f the final temperature, (Q, the heat of reaction, $\overline{c_p}$ a mean specific heat, t the time, A a collision frequency constant, and E the activation energy). Thus, simply by measuring the slope of the curve in Figure 1 at some temperature, and the temperature difference $(T_f - T)$ at that point, k is

determined, and from one experiment the activation energy can be determined.

Some of the important results obtained with the apparatus have been concerned with the hydrazine family of propellants. It was found that the gas-phase decomposition rate of UDMH is faster than that of hydrazine. This indicates that the stabilizing of a liquid UDMH and hydrazine mixture could only be accomplished by altering the surface catalytic effects on hydrazine liquid and vapor, and not by altering the homogeneous gas-phase reaction rate.

In a study of the N_2O_4-hydrazine system, the ractions of NO_2-hydrazine were studied as well as the reactions of the decomposition products of NO_2(NO and O_2) with hydrazine and its decomposition products (NH_3 and H_2). In all, over 16 different reactions were studied. It is of course impossible to review the results of all these reactions; but again it is interesting to note some results of practical significance.

It was found that the reaction of hydrazine with NO_2 proceeds in two steps. The first is a very fast step in which the NO_2 is reduced to NO; the second is a very much slower step in which the NO reacts.

Also, NO was found to have important effects on the H_2-O_2 reaction. In very small quantities, it accelerates the reaction, and in larger quantities it inhibits the reaction. The inhibiting effect could possibly have important consequences in supersonic combustion devices using hydrogen.

With respect to rocket propulsion, perhaps the most interesting finding is that the hydrazine-NO_2 reaction is about 1,000 times faster than the reaction between the decomposition products of both NO_2 and hydrazine. Thus, if in rocket operation the N_2O_4-hydrazine propellant decomposes before reacting, there can be serious performance losses and chamber "pops."

REFERENCES

(1) Eberstein, I., "The Gas-Phase Decomposition of Hydrazine Propellants," AFOSR Technical Report 708, Princeton University, 1964.

(2) Eberstein, I. and I. Glassman, "The Gas-Phase Decomposition of Hydrazine and Its Methyl Derivatives," 10th Symposium on Combustion, Pittsburgh, Pa.: Combustion Institute, 1965, pp. 365-374.

(3) Eberstein, I. and I. Glassman, "Consideration of Hydrazine Decomposition (Catalytic Effects)," Progress in Astronautics and Rocketry, Vol. 2, "Liquid Rockets and Propellants," New York: Academic Press, 1960, pp. 351-366.

(4) Sawyer, R. F., "The Homogeneous Gas-Phase Kinetics of Reactions in the Hydrazine-Nitrogen Tetroxide Propellant System," AFOSR Technical Report No. 66-0855, Princeton University, 1966.

(5) Sawyer, R. F. and I. Glassman, "The Gas-Phase Reactions of Hydrazine with Nitrogen Dioxide, Nitric Oxide, and Oxygen," 11th Symposium (International) on Combustion, Berkeley, California: Combustion Institute, 1966, pp. 84-85.

high-altitude tethered balloons

THOMAS KELLY, Aerospace Instrumentation Laboratory, AFCRL

The feasibility of tethering balloons at altitudes above 60,000 feet is being studied by AFCRL balloon engineers. This possibility is suggested as the result of encouraging experiments with a 10,000-foot tethered system, a detailed analysis of upper-level climatological conditions, and by recent "breakthrough" progress in fiberglass cable technology by both the Navy and industry.

Stratospheric tethered-balloon systems would likely have broad scientific and military utility if the current use of lower-altitude tethered balloons is any index. If one discounts the thousands of World War I and World War II barrage balloons, and the unnumbered children's circus balloons, the use of low-altitude tethered balloons is at an all-time high.

Current scientific experiments using tethered balloons range from studies of atmospheric diffusion and electrification and structure to a determination of antenna patterns in a near-free-space environment. Engineering of functional test uses during the past year have ranged from the development of the Surveyor lunar soft-landing system to the measurement of blast effects at low altitude, and to the functional testing of equipment having direct limited-war application.

While most experiments have been limited to altitudes below 5,000 feet, some have been extended to nearly 20,000 feet. As

might be expected, the extension of the balloon capability to a higher altitude would contribute little to the effectiveness of many experiments. However, the availability of a stable, vibration-free platform above the tropopause would greatly enhance the range and value of other tests and experiments.

AFCRL began the study of high-altitude tethered baloons in 1965. A developmental goal of a 10,000-foot altitude and 300-pound payload was established as applicable to a broad range of test requirements. Using a spherical balloon tethered by a steel cable, a balloon system that performs well in winds of more than 20 knots was developed. Concurrently, the study of elements of the more ambitious high-altitude system was initiated. Such studies included surface and upper-level climatology to 100,000 feet for various locations, consideration of a wide range of balloon-vehicle configurations, and assessment of the problems of producing an aerodynamically shaped tethering cable from high-strength materials.

The performance of various possible tethered-balloon systems has been programmed for digital-computer analysis. This analysis involves balloon systems which employ differing tether-cable materials, shaped and cylindrical cross-section cable, a variety of balloon configurations, and a number of model atmospheres. This will permit consideration of the many possible trade-offs between these factors.

At this point, the feasibility of very-high-altitude tethering has not been established. Feasibility, however, is really a matter of perspective. If we restrict the use of a tethered-balloon system to a quiescent atmosphere, as, for example, the arctic in the summer, a relatively simple and inexpensive system is no doubt possible. If we consider an unfavorable atmosphere, such as that of Japan in the winter, any tethered system is likely to be unworkable. Because the atmosphere is not uniformly friendly or hostile to tethered balloons, present studies are being concentrated on the climatological, physical and economic limitations imposed upon tethering by the real atmosphere.

atmosphere in a computer

UPPER ATMOSPHERE PHYSICS LABORATORY, AFCRL

The atoms and molecules of the upper atmosphere are characterized by a continuous chemistry of interaction and reaction sustained by solar energy. The brief interval of a solar eclipse, for example, profoundly affects the rate of association, dissociation, recombination, ionization, and deionization of atmospheric species. The pattern of reactions changes markedly with time of day, latitude and season.

Between altitudes of 60 to 120 km, the dominant elements making up the atmospheric gas are oxygen and nitrogen. These two elements are found in many combinations, such as O^-, O_2^+, NO_2^-, N_2O, and so on. Reaction rates among these oxygen-nitrogen species are governed by many factors--temperature, mean free paths, and concentrations of the various species.

How do reaction rates vary with altitude and with radiation intensity? In a report soon to be published, "A Technique for Solving the General Reaction-Rate Equations in the Atmosphere," (AFCRL-67-0221), Thomas J. Keneshea of AFCRL discusses a computer model which helps provide answers to these questions. The model deals only with 168 possible photochemical reactions that can take place among 15 oxygen-nitrogen species, plus free electrons. The model gives the researcher a powerful tool for studying reaction rates in the upper atmosphere under a variety of controlling influences. Because of the complex nature of atmospheric gas reactions, computer modeling affords the best available method for conducting such studies.

The model involves, fundamentally, the solution of an extensive set of simultaneous nonlinear first-order differential equations. The method adopted by Keneshea contains two important features. First, the integrating increment is allowed to change freely as the calculation advances so that the solution over a long period of time can be obtained.

Next, a means is provided for calculating the accuracy of the solution so that the accumulation of errors can be controlled.

The present computer model represents an extension of work in progress by Keneshea and others since 1962. The most significant change in the present model is the handling of the solution for a species after it has gone into equilibrium or into quasi-equilibrium with one or more other species. Algebraic equations used previously were inadequate to handle this basic problem. Keneshea has developed a set of exponential equations to replace the previous algebraic equations.

One problem that has been overcome--seemingly a simple one, but one that the computer had trouble coping with--was the situation where one dominant ion species was superseded by another dominant ion species. When this happened, the limit of allowable charge imbalance was exceeded, and the program was incapable of advancing the solution.

The computer model has been used to study the behavior of the atmosphere under scores of varying conditions--diurnal variations of charged species and neutral species at a given latitude and at various altitude strata, nuclear-weapons effects in which the solution starts with high initial electron concentrations and incorporates a continuing source of electrons, the effects of sunlight reflected from clouds and oceans on D- and E-layer ionization, and the variability of the atmospheric composition under eclipse conditions.

The solutions reached by the computer model have been tested against observational data by rocket probes and are in close agreement at E-region altitudes. In the D region, comparison of the computer models with experimental profiles indicates that the chemistry of this region requires considerably more study. ✪

THE LASER AS A LIGHT SOURCE FOR STUDYING IMPERFECTIONS IN CRYSTALS

CAPTAIN RICHARD C. POWELL, Solid State Sciences Laboratory, AFCRL

The study of light scattering has been an important area of research for many years for those working with liquids and gases. However, because of the extremely low scattering power, light scattering has not been used as successfully by solid-state researchers. Recently, the development of the laser has produced new interest in the study of light scattering in solids. One reason for this is that the use of a laser provides a very powerful light source which helps to alleviate the problems associated with the low light-scattering power. Another reason is that the scattering of light by a crystal is of great importance in determining the quality of the crystal for use as a laser.

We have recently initiated a program to study the scattering of light by single crystals using a laser as a light source. The program has two goals: first, to determine the usefulness of light scattering as a means of studying crystal structure; and second, to correlate the light-scattering properties of a crystal with its device properties when used as a laser.

The apparatus we are using employs an electro-optical 1mw He-Ne ($\lambda = 6{,}328$Å) laser as a light source. The light is focused at the interior of the sample by a scanning microscope. Two methods can be used to investigate the light-scattering characteristics of crystals: single-particle scattering, and total scattering. For studying single-particle scattering, the scattered light is generally observed and photographed through a vertical microscope at 90^{o} to the incident beam of light. The incident beam of light is scanned in a horizontal plane to illuminate an area of the sample comparable to the field of view of the microscope. This type of scattering can be studied as a function of sample orientation, position within the sample, and polarization. Single-particle scattering (without beam scanning) can also be observed in the horizontal plane at 45^{o}, 90^{o}, and 135^{o} from the incident beam. Small-angle single-parti-

cle scattering can be observed by focusing the main part of the light beam after it has passed through the sample onto a black wire. The effect of temperature on vertical single-particle scattering can be studied by placing the sample in a 108-watt Kanthal wound furnace.

For studying total scattering, the observing microscope is mounted in the horizontal plane, the intensity of the scattered light is detected by an RCA 1P28 photomultiplier tube, and the results are recorded on a strip-chart recorder. The samples are immersed in a liquid with the same refractive index to decrease the amount of surface scattering by the sample. Total scattering can be measured as a function of scattering angle for different sample orientations, different positions in the sample, and different polarizations. It can also be measured as a function of sample orientation at a scattering angle of 90° for different polarizations and different positions within the sample.

By taking pictures of successive planes in the sample, the single-particle scattering studies can give a three-dimensional map showing the number of scattering centers and where they are located within the crystal. Any clustering of defects around dislocations can be observed in this way. Figure 1 is a photograph of an area within a ruby crystal showing numerous scattering centers and a clustering of scattering centers along a small-angle boundary. The plane of observation is a $\{10\bar{1}0\}$ plane, and the incident light beam is oriented along the [0001] direction. Figure 2 shows a similar picture of a different ruby sample. In this sample, there are not as many individual scatterers visible; but there is a region of very strong clustering. Interference patterns can be seen around the scattering regions. The plane of observation of this photograph is a $\{10\bar{1}0\}$ plane, and the direction along which the incident beam is aligned is an $[11\,\bar{2}0]$ direction.

Figure 1. Scattering centers in a ruby crystal showing clustering along a small-angle grain boundary.

Recently, an attempt was made to give single-particle scattering a more quantitative basis.(1) By calibrating the scattering power of individual scatterers versus the scattering power of polystyrene-latex suspension in water, the size of the scattering centers was determined in terms of equivalent latex diameters. This circumvented the problem of determining the unknown refractive index of the scatterers. Another possible way to

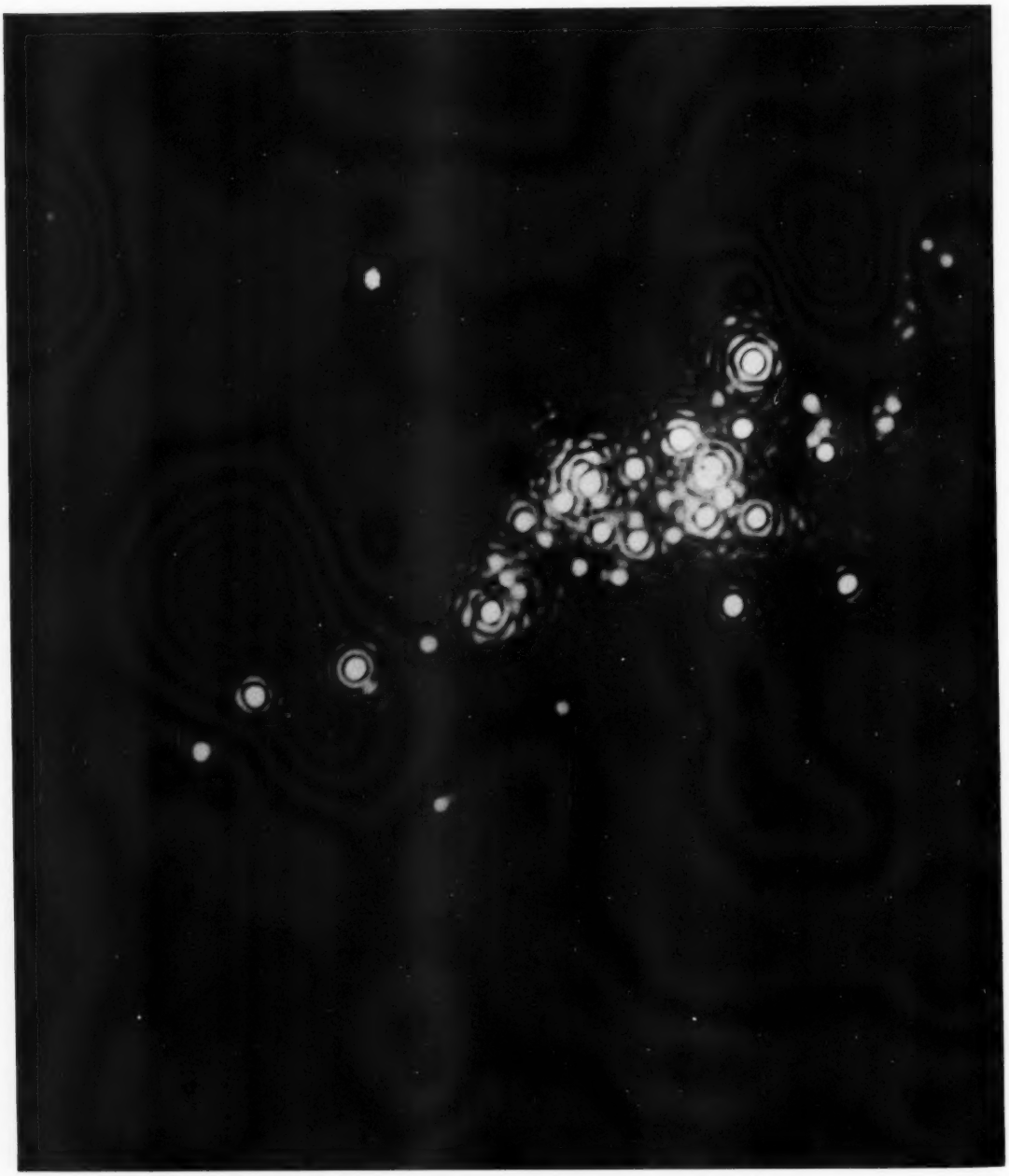

Figure 2. Region of intense scattering in a ruby crystal.

determine the size and refractive index of single-particle scatters is to measure their scattering power at several angles and compare the results with those predicted by Mie's scattering theory.

Total scattering experiments show how light is scattered by a volume of the crystal which may include light scattered by individual scatterers which are too small to be seen in single-particle scattering. Figure 3 shows the results of measurements of total scattering power versus scattering angle (2θ) for a ruby laser rod with the cylinder axis corresponding to the c-axis of the crystal. The results for the volume element shown here displayed a pronounced orientation effect. The sample orientation of $\phi = 0^{o}$ corresponded to an $[11\bar{2}0]$ plane being parallel to the incident light beam. The angular dependence of scattering power has a distinct peak at $2\theta = 90^{o}$ for $\phi = 45^{o}$ which is not present at $\phi = 0^{o}$. Figure 4 shows the dependence of scattering power versus sample orientation at $2\theta = 90^{o}$ for the same volume element of the sample. The results show a peak at $\phi = 45^{o}$.

The results are consistent with those predicted by the theory of scattering from cylindrical regions of clusters of point scatterers. Similar result have been observed in some alkali-halide single crystals.(2) From these measurements, it should be possible to determine the effective size, shape, number, and orientation of these scattering regions along with the concentration and polarizability of the point scatterers within the scattering regions.

In many parts of the samples, no peak

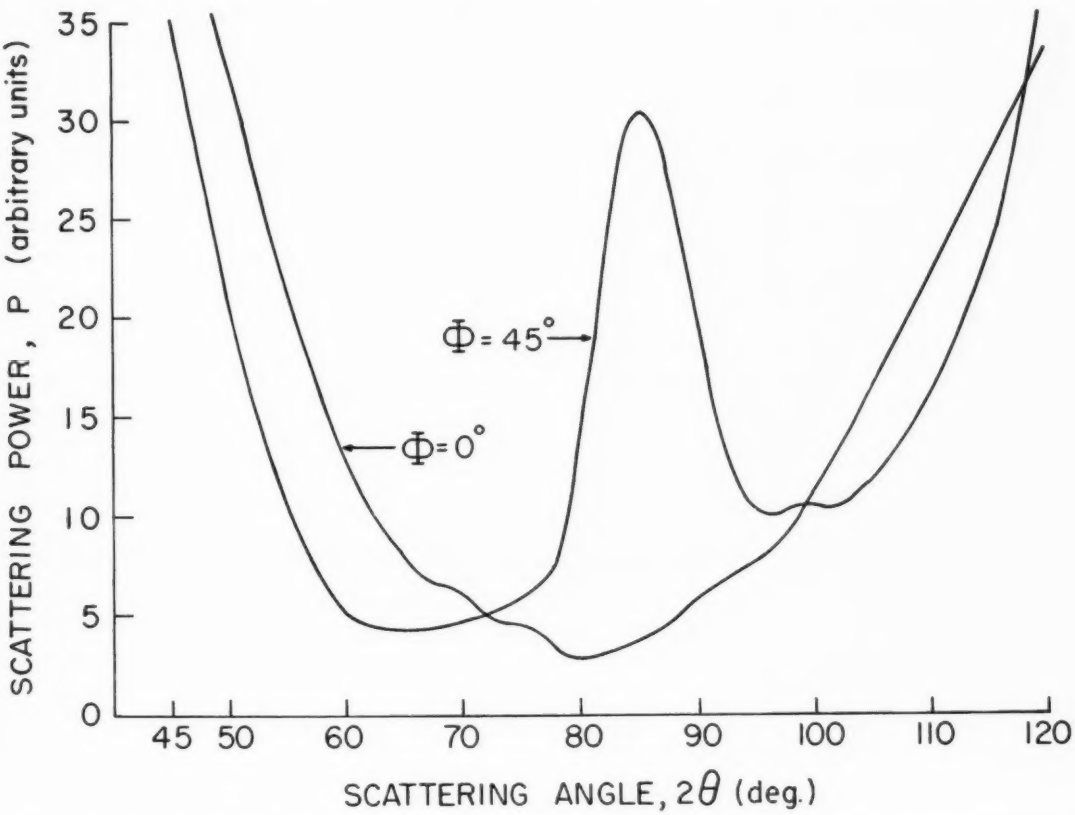

Figure 3. Angular dependence of the light scattering of a ruby rod. Φ is the angle of rod orientation, $\Phi = 0^{\circ}$ corresponds to an $[11\bar{2}0]$ direction parallel to the beam, polarization $\perp, \perp$.

occurs in the angular dependence of scattering power. This indicates the scattering regions are spherical, and the well-known Rayleigh-Gans theory(3) can be used to interpret the results. Quantitative theoretical predictions are made difficult by the presence of scatterers of varying size and refractive index.

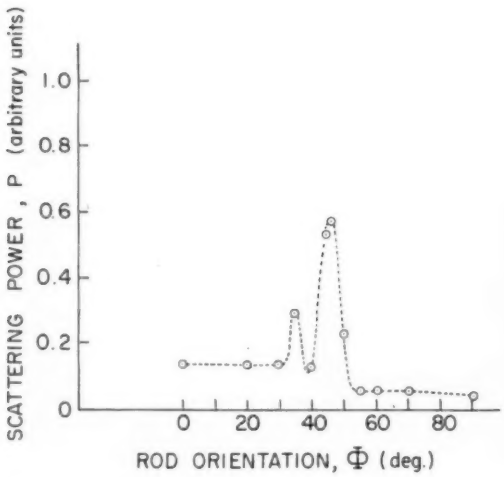

Figure 4. Dependence of light scattering of a ruby rod on rod orientation at $2\theta=90°$. $\Phi=0°$ corresponds to an $[11\bar{2}0]$ direction parallel to the beam, polarization $\parallel$, $\parallel$.

As we obtain a better understanding of this new experimental technique, it is hoped that light scattering will provide both a different method for studying crystal defects and a way to evaluate material as to its ability to be used for lasers. ✪

REFERENCES

(1) Vand, V., K. Vedam and R. Stein, J. Appl. Phys., 37, 2551, 1966.

(2) Sibley, W. A., Phys. Rev., 132, 2065, 1963.

(3) van de Hulst, H. C., Light Scattering by Small Particles, New York: John Wiley & Sons, Inc., 1957.

Captain Richard C. Powell, a physicist with the Purification and Growth Branch, Solid State Sciences Laboratory, AFCRL, has a B.S. (1962) from the United States Naval Academy, and an M.S. (1964) and Ph.D. (1966), both in Physics and both from Arizona State University, Tempe, Arizona. He is presently concerned with the growth and characterization of electronically active single crystals. Specifically, his interests lie in the nondestructive evaluation of laser materials by means of coherent light-scattering techniques, as well as ion-interaction studies in crystals. Captain Powell is a member of the American Institute of Physics.

Isobaric Spin....its influence on research in nuclear physics with small accelerators

DR. GALE I. HARRIS
General Physics Research Laboratory, ARL

The concept of isobaric spin was introduced into nuclear physics by W. Heisenberg(1) 35 years ago, and was soon developed in detail by E. P. Wigner(2) as a convenient formal method of accounting for the 2 charge states of the nucleon. The mathematical formalism for isobaric spin was devloped in complete analogy with the (by that time) familiar quantum-mechanical formulation of ordinary (mechanical) spin. A subtle difference, however, is that ordinary spin can be related to co-ordinates in ordinary space, whereas isobaric spin must be dealt with in terms of co-ordinates in an abstract charge space. Thus, although isobaric spin is, from

a formal point of view, no more complex than ordinary spin, it is a more elusive conceptual property of nuclear-energy levels.

The isobaric spin ($\vec{t}$) of a nucleon is assigned the value $t = 1/2$. The proton and the neutron are then distinguished by the two projections (t_z) of $\vec{t}$ along a z-axis in charge space. A neutron corresponds to the projection $t_z = +1/2$, and a proton to $t_z = -1/2$. Just as the total ordinary spin of a system consisting of several nucleons is the (vector) sum of the spins of the individual nucleons, the total isobaric spin $\vec{T}$ of a system is the vector sum of the isobaric spins of the individual nucleons. That is, $\vec{T} = \sum_i \vec{t}_i$, where i labels the nucleons. Similarly, the z component (T_z) of the total isobaric spin of a system is just the (algebraic) sum of the t_z of the individual nucleons. This sum is equivalent to $T_z = (N - Z)/2$, where N and Z are the number of neutrons and protons, respectively, in the nucleus. It is evident from this that all the energy levels of a given nucleus will have the same z-component of total isobaric spin T_z, but in principle they can have any value of $\vec{T}$ for which $T_z \leq T \leq (N + Z)/2$ is satisfied.

A direct consequence of isobaric-spin formalism is the concept of isobaric-spin multiplets in nuclei. That is, in a series of nuclei, each having the same total number of nucleons but different values of T_z, there should exist a series of $2T + 1$ nuclear-energy levels ("isobaric-analog states") of successively increasing charge but with identical nuclear wave functions. The successive members of the multiplet correspond to the successive conversions of a neutron into a proton. Sets of nuclei having the same total numbers of nucleons are known as "isobaric nuclei"--hence, the origin of the name "isobaric spin" for the quantum number which labels the multiplet of isobaric-analog states spread through the set of isobaric nuclei. Each member of the multiplet corresponds to a different projection T_z of the isobaric spin $\vec{T}$ along the z-axis in charge space. There are $2T + 1$ possible projections of $\vec{T}$. Hence, each multiplet consists of a level in each of $2T + 1$ isobaric nuclei. Such a multiplet for $T = 3/2$ in the mass-31 nuclei is shown schematically in Fig. 1. One could expect, then, that each energy level of a given nucleus should have associated with it a value of the isobaric spin $\vec{T}$ in addition to the usual quantum numbers energy, ordinary spin, and parity.

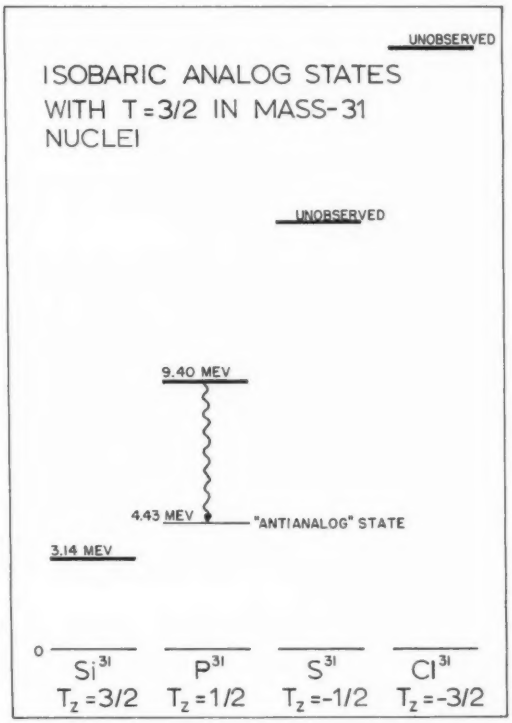

Figure 1. Schematic representation of $T = 3/2$ isobaric-analog states in the mass-31 nuclei. The upward displacement of the analog states (heavy lines) from one nucleus to the next is due to the additional charge associated with the successive conversion of neutrons to protons. The antianalog state in P^{31} discussed in the text is shown.

A very important condition, however, for isobaric spin to be a meaningful concept is that the nuclear forces must be charge-independent. Formally speaking, for $\vec{T}$ to be a "good" quantum number, it must commute with the nuclear Hamiltonian. There is a term in the Hamiltonian, however, which is manifestly charge-dependent. This is the Coulomb interaction term due to the proton

charges. Thus, it was felt for many years that it is meaningful to talk of isobaric spin only in the very light nuclei in which the total proton charge is a small effect relative to the pure nuclear forces. In medium and heavy-weight nuclei, in a nucleus with Z protons, the isobaric analog of a low-energy level in a neighboring Z-1 nucleus will lie at a very high excitation energy due to the interaction of the charge of the added proton with the total charge of the Z-1 nucleus. At such high energies, the energy-level density is very high (nearly a continuum), and the isobaric-analog state might be expected to be "dissolved" into the continuum of ordinary compound-nucleus levels and thus be unobservable.

Consequently, the experiments (3) of Anderson, et al., at the Lawrence Radiation Laboratory in 1961-62, in which they observed well-defined isobaric-analog states in several medium-weight nuclei superimposed upon a "continuum" of compound-nucleus levels by studying the neutrons emitted following bombardment with 14.8 MeV protons, came as a considerable surprise. Since that discovery, the interest in isobaric-analog phenomena in nuclear-structure physics has increased enormously. Many other similar cases have now been studied extensively in medium-weight nuclei with tandem accelerators. The theory of such phenomena is now well developed, in large part due to the efforts of Dr. Robson(4) at Florida State; and it is reasonably well understood why such analog levels should be observed in spite of the very large Coulomb forces.

Concurrently with these developments in medium-weight nuclei, very strangely behaving resonances in the medium-light nuclei between mass 27 and 40 were being observed and studied in the Aerospace Research Laboratories, and at the University of Utrecht, Holland, with small 2-3 MeV accelerators. The first such resonance was observed at ARL in 1963, and reported(5) in 1964, in a high-resonance yield of gamma rays from P^{31} when Si^{30} targets were bombarded with protons with an energy of 2.187 MeV. Detailed measurements showed that this resonance was almost a pure single-nucleon state. That is, roughly speaking, it consists of a nucleon in a pure "parking orbit" about an inert mass-30 core. The nucleon has 3 units ($\hbar$) of orbital angular momentum, and is coupled with its ordinary spin in such a way that the total spin of the nucleus is 7/2 with odd parity. That a level with such high orbital angular momentum and at such low bombarding energies should occur as a strong resonance was, in itself, a very surprising fact. More surprising, however, was the way in which the resonance behaved in its decay by the emission of gamma rays. Hundreds of resonance levels in nuclei in this mass range have been studied, where decay is to the ground state or, in complicated ways, to several excited states. This particular resonance, however, broke the usual pattern by decaying completely to a single, rather high-energy state in P^{31}. This state, which lies at 4.43 MeV excitation in P^{31} (see Fig. 1), was shown to have the same ordinary spin and parity as the resonance level by means of angular correlation and gamma-ray polarization measurements.

It is now known that this resonance level ir P^{31} is the isobaric analog of an almost pure single-particle state at 3.14 MeV excitation in the Si^{31} nucleus. From the theory of isobaric-analog states and their multiplet character, we know that the resonance has $T = 3/2$, and can be described as a state which exists one third of the time as a proton in orbit about an inert Si^{30} core, and two thirds of the time as a neutron in orbit about a P^{30} core. The lower state at 4.43 MeV can be similarly described as a state with $T = 1/2$, and with the same wave function as the resonance except that it is two thirds of the time a proton, and one third of the time a neutron about inert Si^{30} and P^{30} cores, respectively. This lower state is an excellent example of what is now sometimes referred to as an "antianalog state." The energy separation between the analog state and its antianalog is a direct measure of the isobaric-spin dependent part of the force between nucleons in complex nuclei. Furthermore, the absolute position of the two states gives a direct measure, when combined with similar data from neighboring nuclei, of the over-all average interaction

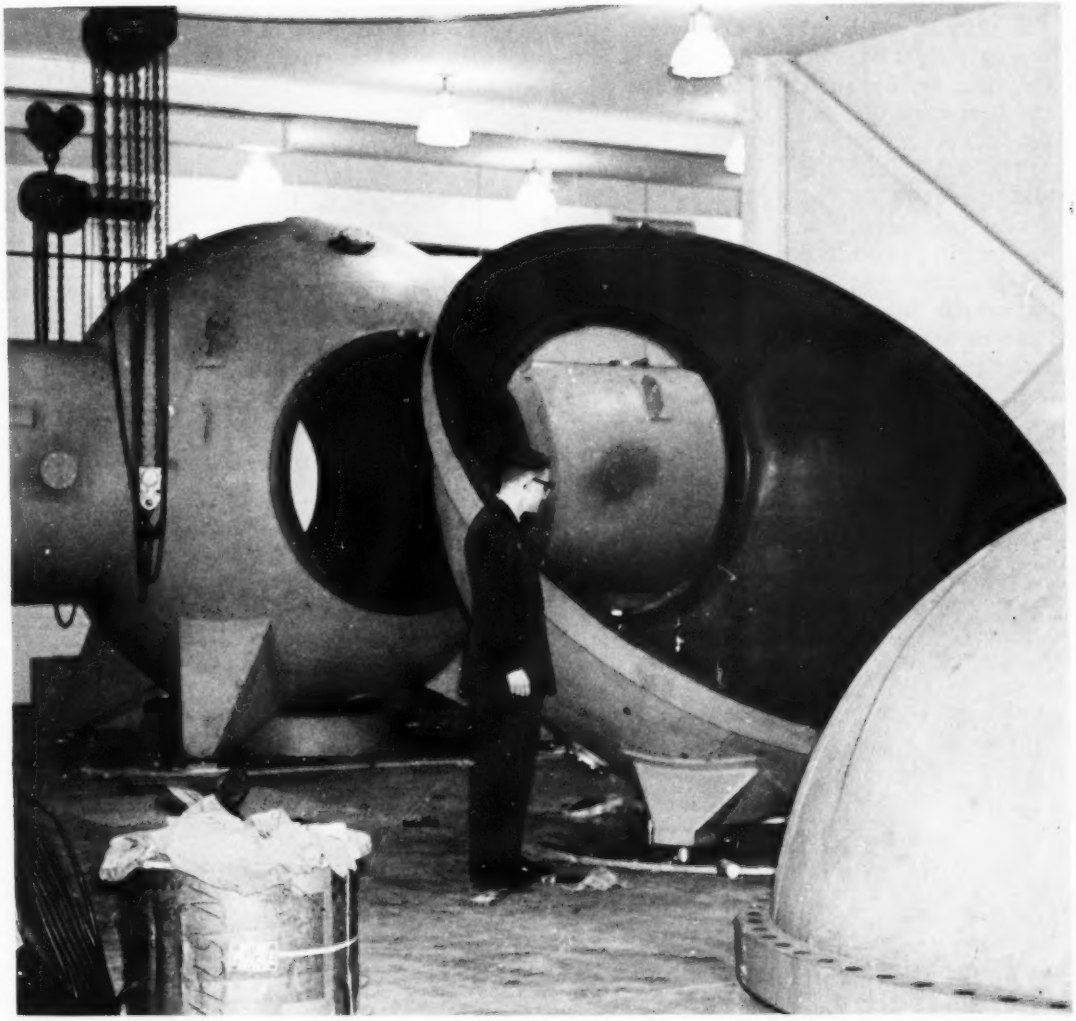

Figure 2. The 8-MeV ICT Tandem Accelerator during assembly at the Aerospace Research Laboratories.

energy between pairs of nucleons in different orbits. Similar, and in some cases even more informative, examples of analog and antianalog states have subsequently been discovered and studied in the ARL Nuclear Structure Physics Laboratory in P^{30}, Cl^{35}, and Cl^{37}. (6, 7, 8)

The importance and expected behavior of isobaric-analog states in medium-light nuclei, and their capability of being studied even with the small accelerators, were first enunciated by Professor P. M. Endt of Utrecht University at an International Symposium on Low-Medium Mass Nuclei held at ARL in 1966. He pointed out that such resonance states should, in favorable cases, show up in proton-capture reactions as strong resonances which have:

a. A large probability of proton capture (or proton emission).
b. A high probability of gamma-ray emission.
c. A simple gamma-ray decay to a single lower state--the antianalog state.

All this is caused by the single-particle analog character of the resonance. He cited the ARL examples in P^{31} and Cl^{35} as two of the best examples then known in which these conditions are met.

The systematic study of isobaric-analog states is now in the process of providing a very considerable body of new information on the structure of complex nuclei and on nuclear interactions. This includes the isobaric-spin dependence of the two-nucleon interaction mentioned above in addition to, for example, questions dealing with the charge-dependence of the nuclear force, the isobaric-mass formula, Coulomb energies of different shell-model orbits, isobaric-spin impurities, and electromagnetic transition rates. Information from these states can also be used in some cases to provide estimates on such gross properties of the nucleus as its over-all shape.

Although an impressive amount of analog-state data has come from the small accelerators, it is also true that, even in the medium-light nuclei, only a few of the lowest-lying analog states can be reached with these machines. The best cases accessible to these machines now appear to have been located and studied. Analog states with higher values of $\overrightarrow{T}$ and in higher shell-model orbits can only be studied with higher-energy accelerators. These higher-lying states and analog states in heavier nuclei will be explored at ARL with the new ICT Tandem Accelerator. Views of this accelerator during assembly at ARL are shown in Figs. 2 and 3.

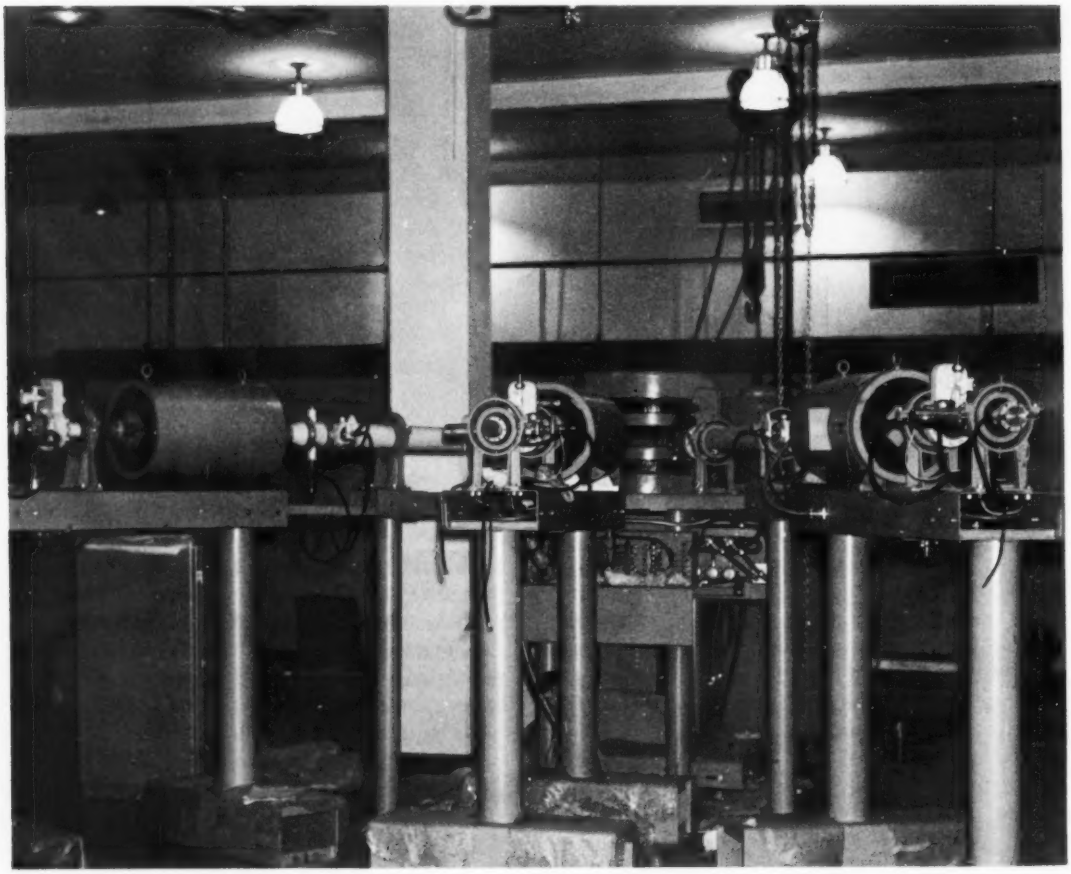

Figure 3. Beam transport system for the ICT Tandem Accelerator during assembly.

REFERENCES

(1) Heisenberg, W., Z. Physik, 77, 1932.
(2) Wigner, E. P., Phys. Rev., 51, 106, 1937.
(3) Anderson, J. D., C. Wong and J. W. McClure, Phys. Rev., 126, 2170, 1962.
(4) Robson, D., Annual Review of Nuclear Science, ed. E. Segre, Vol. 16, 119, 1966.
(5) Harris, G. I., H. J. Hennecke and F. W. Prosser, Phys. Letts. 9, 324, 1964.
(6) Harris, G. I. and A. K. Hyder, Jr., Phys. Letts., 22, 159, 1966.
(7) Watson, D. D., Phys. Letts., 22, 183, 1966.
(8) Hyder, Jr., A. K. and G. I. Harris, Phys. Letts., 24B, 273, 1967.

Dr. Gale I. Harris is a physicist with the General Physics Research Laboratory, ARL, where he is conducting research on nuclear-structure physics of importance to the Air Force. He also heads up a group of nuclear physicists who are presently engaged in a systematic study of the properties of the excited states of medium-light nuclei using the techniques of gamma- and beta-ray sprectroscopy. Dr. Harris serves on OAR's Nuclear Physics Subpanel which formulates Air Force objectives and plans in nuclear physics. He has a B.S. (with honors) in Engineering Physics (1957), an M.Sc. in Physics (1959), and a Ph.D. in Physics (1962), all from the University of Kansas. He is the author or co-author of more than 30 papers in nuclear physics. In 1964, while a first lieutenant in the Air Force, he was named the USAF officer scientist of the year. He also received the USAF Research and Development Award in 1963. Dr. Harris is a member of the American Association for the Advancement of Science, the American Physical Society, Sigma Xi, and Sigma Pi Sigma.

application of high-speed holographic photomicroscopy

EVERETT D. STEPHENS
Thermomechanics Research Laboratory, ARL

A recent article published in the OAR Research Review (Ref. 1) discussed the conclusions from studies on the interaction between science and technology. An example of what might grow out of a given research effort is represented by an ARL jointly supported program with TRW Systems, where the primary objective was an improved understanding of the physical processes involved in the electrification of fluids. Dr. D. B. Langmuir and Dr. R. F. Wuerker were primarily responsible for the direction of the research studies at TRW Systems.

The microscopic electrified fluid streams studied occur at high speed, and are virtually impossible to record with a conventional optical microscope or imaging system. In order to overcome the working-distance and depth-of-field limitations of the classical microscope, a two-step imaging process (holographic photomicroscopy) of high resolution was developed and applied to the study of the electrostatic charging process. In this technique, one first records the optical interference pattern of the "scene," and then uses this record to reconstruct the original scene. The reconstructed scene can be leisurely examined with conventional optical systems of limited object volume.

The new technique makes use of holography with a submicrosecond-duration, Q-switched ruby-laser illuminator of high intensity and coherence. A high-resolution photographic plate is used to record the optical interference pattern between a coherent background wave and the waves scattered from a scene. The developed plate, when reilluminated by a coherent source, recreates the wave originally scattered from the scene. Definition or resolution of the recreated wave is limited either by the wave length of light or by the

aperture of the examining optics, whichever is least. In the charged filament studies, reconstructed images with resolutions of approximately 5 microns were realized from holograms made with apparatus originally mounted before a vacuum port at a distance of approximately 10 centimeters from the axis of the phenomenon. Equally important is the large extent of object space which can be recorded both in depth and length.

The successful holographic microphotography of the high-speed electrified jets was dependent upon the perfection of a short-duration, coherent, pulsed-light source of sufficient intensity to expose the extremely insensitive photographic plates of high resolution. This requirement was satisfied by TRW Systems' independent parallel effort through the development and perfection of a laboratory-constructed Kerr cell switched ruby laser, which was refined into a light source of sufficient spatial and temporal coherence to meet the requirements of holographic microscopy. The perfection of the light source transformed holography from a phenomenon of academic interest to one of extreme practicality.

The practical consequences of pulsed laser holographic photomicroscopy go beyond the requirements of the present application. Reasonable projection would indicate application to scientific studies that involve moving unpredictable phenomena of either uncertain or changing location. Physical applications include terminal and in-flight ballistics, aerosol-size distributions, cloud physics, studies of sprays, and combustion and rocket-exhaust studies, among others.

During the study, TRW Systems discovered that the holographic process is also capable of interferometric measurements. ✪

REFERENCES

(1) Price, W. J., "Concerning the Interaction Between Science and Technology," OAR Research Review, Vol. V, No. 10, Dec 1966, pp. 1-5.

*(2) Wuerker, R. F. et. al., "Research on Electrostatically Charged Droplet Streams," ARL Technical Report (in preparation).**

(3) Brooks, R. E., L. O. Heflinger, R. F. Wuerker and R. A. Briones, "Holographic Photography of High-Speed Phenomena with Conventional and Q-Switched Ruby Lasers," Applied Physics Letters, Vol. 7, No. 4, 15 Aug 1965, pp. 92-94.

(4) Wuerker, R. F., L. O. Heflinger and R. E. Brooks, "Holographic Photography and Interferometry with the Pulsed Solid-State Laser," NAECON Conference, Dayton, Ohio, 18 May 1966.

** This publication includes other references covering TRW Systems — supported holographic photomicroscopy and holographic interferometry.*

ARL's High-Pressure Electrofluid-Dynamic Rig

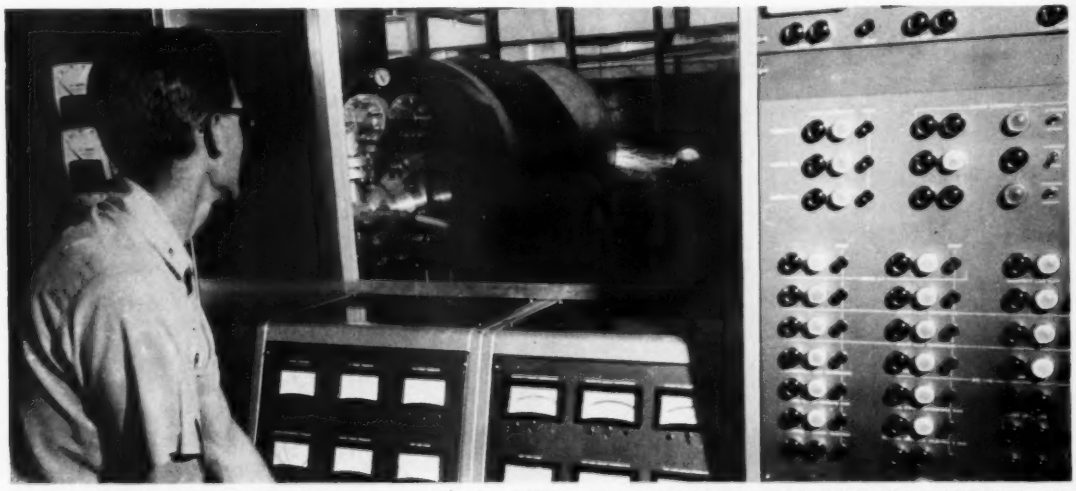

RIG IS BEING OPERATED BY 1ST LT JAMES R. WIFALL OF THE ENERGETICS RESEARCH LABORATORY. NOTE THE "LIGHTNING" PASSING BETWEEN TWO SPHERES ON THE OTHER SIDE OF THE WINDOW.

ORY.
OW.